*17th World Conference on Earthquake Engineering, 17WCEE*
*Sendai, Japan - September 13th to 18th 2020*

# OPTIMAL VISCOUS FLUID DAMPER PLACEMENT FOR SEVICEABILITY LIMIT STATE PERFORMANCE

P.T. Chan(1), Q.T. Ma(2), L. Hogan(3)

(1) *PhD Candidate, The University of Auckland, pcha988@aucklanduni.ac.nz*
(2) *Senior Lecturer, The University of Auckland, q.ma@auckland.ac.nz*
(3) *Lecturer, The University of Auckland, lucas.hogan@auckland.ac.nz*

## *Abstract*

Viscous dampers enhance the seismic performance of buildings by increasing the capacity for damping. It remains a challenge to decide on the optimum placement for the added dampers and it has been a continuing subject of research. In this paper, a new damper placement optimisation algorithm is compared against currently available methods through case studies. The case studies are based on an 8-storey reinforced concrete frame buildings with varying plan asymmetry. The buildings are designed to initially meet the design requirements of typical buildings in a moderate seismic zone in New Zealand. The algorithms then automatically develop damper placement schemes, and subsequently the buildings are evaluated for their seismic performance in terms of typical engineering demand parameters (EDPs) such as inter-storey drift ratio and peak floor acceleration under serviceability limit state earthquake actions.

*Keywords: Optimal Damper Design, Viscous Fluid Dampers, Serviceability Limit State, Buildings with asymmetric plan*

## 1. Introduction

Different existing viscous damper placement optimisation technique can result in drastically different placement designs for the same building. Even for a specific damper placement method, the placement design may still be highly sensitive to the user-selected objective function, ground motion input into the process, and structural characteristics variations. The objective function for the optimisation damper placement problems can be the structural response (e.g., inter-storey drifts, inter-storey velocities, base shear and roof displacement, etc.), or a weighted function of these and other parameters (e.g., seismic loss) [1-3]. Time history analyses are often relied upon to obtain structural response [4]. Other research has adopted the sum of the transfer function amplitudes as the objective functions, thus developing objective functions that are independent of ground motions and overcomes the contentious task of ground motion selections [5-6].

As hinted, different placement optimisation technique can be highly sensitive to the specific ground motion input [7]. Two common approaches to overcome this include using three or more spectrum compatible ground motions as the input and selecting the most frequently occurring damping coefficient at each floor as the final damper placement [8]. Another is to conduct the analyses with seven ground motion records and used the median damper coefficient of each storey as the final damper placement [9].

Moreover, past research had shown that vertical and plan irregularity can greatly affect the behaviour of the damper placement optimisation techniques [10]. Studies that systematically explore this remain scarce [8-9].

This study aims to investigate the effectiveness of a proposed optimum placement design algorithm. Specifically, it will compare how the proposed algorithm performs against other commonly used techniques on a building with varying eccentricity. This study will compare the efficiency of the different techniques by reporting on the number of iterations required, and overall computation effort within the optimisation process.

## 2. Element Exchange Search Algorithms

### 2.1 Element Exchange Method (EEM)

Element Exchange Method (EEM) is a technique originally devised for structural topology optimisation [11]. In that application, EEM removes the least utilised structural element and adds the removed element to the highest utilised location in each iteration, and this is repeated until there is little change to the overall outcome. In the same way, starting from a uniformly distributed arrangement, this research applies EEM concept to relocate viscous dampers in the storey with the lowest objective function to the storey with the highest objective function, and this is repeated until there is no further change in the overall objective function.

Applying this to the damper-positioning problem, peak inter-storey drift ratios are the objective functions to minimise, and the total of damping coefficient for all floors is the constraint. Thus, the EEM process is as follows:

1. Uniformly distribute viscous dampers such that they sum to a constant total viscous damping.
2. Carry out dynamic analysis (e.g. time history analysis) to evaluate the objective function (i.e. the maximum of peak inter-storey drift ratios across all floors for this study).
3. Check the inter-storey drift ratios and move one damper from the storey with minimum drift ratio to that with the maximum.
4. Repeat step 2 and 3 until the objective function of the next iteration is converged.

Algebraically, the optimisation problem can be expressed as follows:

$$\min \max\{(\delta_1)_{max}, \cdots (\delta_n)_{max}\}\text{ , variables : } c_1, \cdots c_n$$

$$\text{s.t. } \sum_{i=1}^{n} c_i = C \qquad (1)$$

$$c_i \geq 0, \qquad i = 1, \cdots, n$$

$$c_i \in \{0, c, 2c, \cdots pc\}$$

where $(\delta_i)_{max}$ is the maximum inter-storey drift ratio of $i$ th story, $n$ is total storeys, $c_i$ is the damping coefficient at $i$ th story, $c$ is a unit of damping provided by a single damper, $C$ is the constraining sum of damping coefficients, p is an integer greater than zero.

Whilst the above describes a unit of damping ($c$) as provided by a single physical damper, this could also be taken as the smallest resolution of damping being reallocated.

### 2.2 Inverse Element Exchange Method (IEEM)

A drawback of the EEM method is that it does not consider the effectiveness of the new damper placement at the next iterative step in the current step. This has a greater potential to lead to a path-dependent optimum solution. This study proposes an improved technique, named Inverse Element Exchange Method (IEEM) to overcome these drawbacks. IEEM considers all possible relocation options and implements the option that offers the maximum improvement in each iteration. This effectively implements the steepest gradient search of the objective function at each iteration. The EEM procedure is as follows:

1. Uniformly distribute viscous dampers such that they sum to a constant total viscous damping.
2. Carry out dynamic analysis (e.g. time history analysis) to obtain the objective function (i.e. the maximum



 

of peak inter-storey drift ratio across all floors).

3. Systematically relocate one damper from the storey with the minimum drift ratio to all other storeys. Each configuration is a potential candidate to be adopted for the next iteration. If the building has *n* storeys, the number of candidate damper configurations is *n*-1.
4. Carry out dynamic analysis (e.g. time history analysis) for all candidate damper configurations and evaluate the objective functions (i.e. the maximum of peak inter-storey drift ratios across all floors) corresponding to all candidate configurations.
5. Proceed with the candidate damper configuration that minimises the objective function for the iteration.
6. Repeat step 2 to 5 until the objective function of the next iteration is converged.

The optimisation problem of IEEM is identical to EEM mathematically and is expressed in Eq. (1). The difference lies in the steps in solving the optimisation problem.

## 3. Case Study Building and Ground Motion Selection

### 3.1 Case study structure

This study adopted an 8-storey reinforced concrete (RC) moment-resisting frame (MRF) building as the prototype building. The building was designed according to New Zealand standards [12-13] and based on the New Zealand 'red book' [14]. The plan and elevation of the building are as shown in Fig. 1 and Fig. 2. The centre of mass (CM) of the structure was deliberately varied to test the optimisation routine's effectiveness against symmetric and asymmetric structures. It was decided to vary the CM rather than the centre of rigidity (CR) as it would otherwise introduce significant structural changes that make the comparison difficult. Three cases were considered,

i) Symmetrical case - the CM and CR are both centrally located,

ii) One-way asymmetrical case - the CM is offset by 20% in the y-direction for all floors, and

iii) Two-way asymmetrical case - the CM is offset by 25% in the x-direction and 20% in the y-direction for all floors.

These configurations are shown in Fig.1 (a) – (c), where L1, L2, L3 and L4 represent bays which viscous dampers can be allocated. The height of each storey is 3.3 m.

The column sections varied as a function of the building height. The external dimensions of the columns are as shown in Fig. 2. As the structure is symmetrical, Fig. 2 only denotes column section sizes for only one-half of building for clarity. Moreover, Fig. 2 only shows the column sections for the exterior frame. The interior columns have a 500 mm by 500 mm cross-section, over the building height, and are only gravity bearing. The material of concrete and rebar, as well as the dimension of beam and slab, are shown in Table 1 and Table 2 respectively. Rigid diaphragms on each floor are assumed for all case study buildings. The case study buildings are modelled in SAP2000 [15].

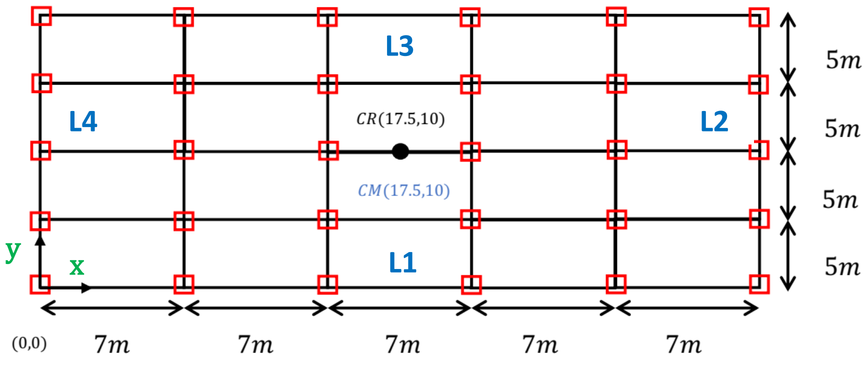


(a) The symmetric plan

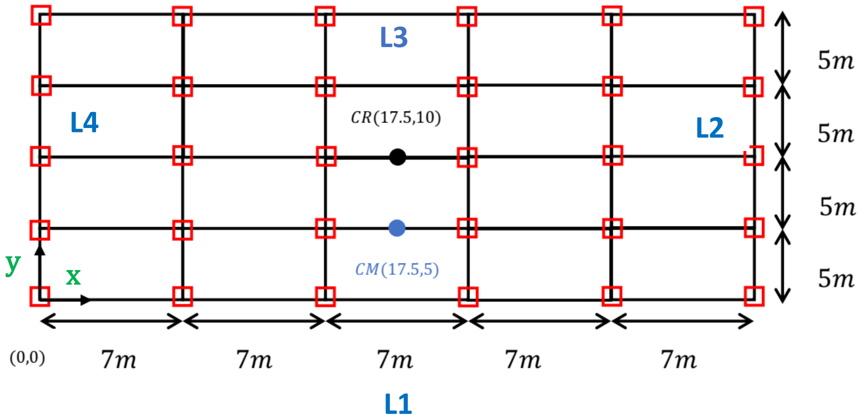


(b) The one-way asymmetric plan

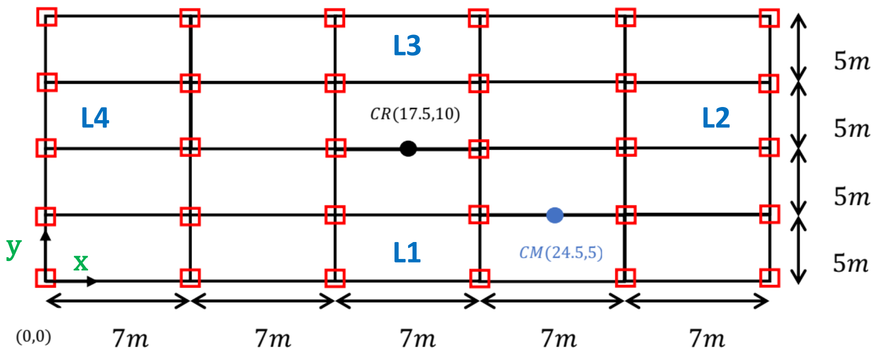


(c) The two-way asymmetric plan

Fig. 1. The plan of the case study structure

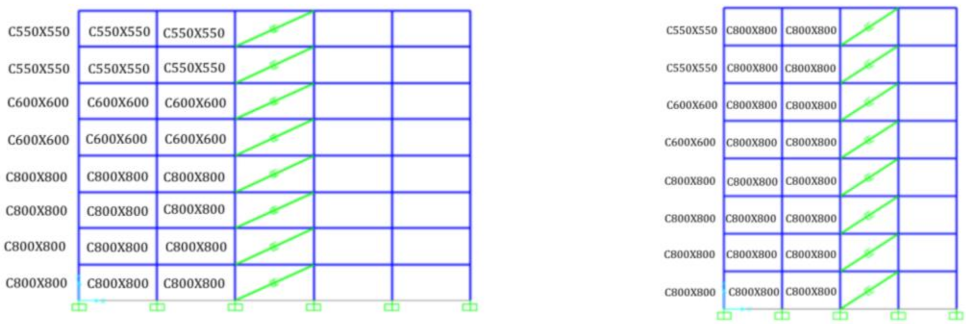


Fig. 2- The elevation of the case study structure



 

Table 1–Material properties

| Material | Strength |
|---|---|
| Rebar | $f_y = 500\ MPa$ (Gr500E) |
| Rebar (for shear and confinement) | $f_y = 500\ MPa$ (Gr300E) |
| Concrete | $f_c' = 40\ MPa$ |

Table 2– Dimension of beam and slab

| Section | Size |
|---|---|
| External Beam | $600 \times 400\ mm$ |
| Internal Beam | $400 \times 300\ mm$ |
| Slab thickness | 150mm |

### 3.2 Ground motion selection

Ten pairs of ground motion records were selected from the Pacific Earthquake Engineering Research (PEER) Centre's NGA database [16]. The ground motions were selected according to magnitude, fault-to-site distance and site condition to match a representative site in Christchurch, New Zealand. The pre-scaled magnitude of these ground motions varied from 6.5 to 7.9 and these selected ground motions were recorded at 22-198 km from fault rupture, on NZS1170 site class C equivalent soil. The selected ground motions were scaled to the target spectrum at serviceability limit state over the period range of interest based on NZS1170.5. The pairs of ground motion are applied to the analysis as acceleration in the principal axes, these are subsequently swapped to ensure both combinations of ground motion directions are tested. This resulted in 20 time history analyses for each test since each pair of ground motion records has two orthogonal components which are exchanged for application along x and y directions.

## 4. Comparison of Proposed Methods with Existing Methods

This study adopts seven existing techniques as a benchmark for the two new proposed methods. The existing techniques are namely,

i. Simplified Sequential Search Algorithm (SSSA),

ii. Genetic Algorithm (GA),

iii. Distribution based on Story Shear Strain Energy (SSSE),

iv. Distribution based on Story Shear Strain Energy to Efficient Storeys (SSSEES) as proposed by Hwang (2008) [17],

v. Distribution based on Energy Dissipated by Viscous Dampers (EDVD),

vi. Distribution based on Energy Dissipated by Viscous Dampers to Efficient Storeys (EDVDES) proposed by [10], and

vii. Uniform Distribution (UD).

All methods adopted the same total damping coefficient as a constraint for the damper placements. The authors acknowledge that it is not possible to include all technique. The optimisation routine relied on SAP2000 for the structural analyses, and a MATLAB script interacted with SAP2000 using the open application programming interface (OAPI).

### 4.1 Existing methods used in the case study

#### 4.1.1 Simplified Sequential Search Algorithm (SSSA)

SSSA [3] minimises EDPs by allocating dampers sequentially to the storey with the maximum weighted function of inter-storey drifts and velocities (the objective function). In this study, the objective function of SSSA is the maximum peak inter-storey drift ratio along the building height. The constraint of SSSA is the total damping coefficient which is consistent with other methods.

#### 4.1.2 Genetic Algorithm (GA)



 

Genetic Algorithm optimises the problem by five key steps: (1) Setting the initial population composed of a number of chromosomes making the algorithm have initial candidate solutions (2) determining the fitness function of all the population (3) Selecting the chromosomes with better fitness function to the crossover pool (4) Crossover making the selected chromosomes have probability to do crossover with each other (5) Mutation allowing the genes of chromosomes to have probability to mutate. The GA application for this particular study adopted 50 initial populations, Roulette Wheel Selection (RWS) as the selection strategy, 70% crossover probability and 20% mutation probability for the GA. The objective function is combined with the penalty function as the fitness function shown below:

$$\Phi = f_{obj} + p \tag{2}$$

$$f_{obj} = \max(\delta_x)^2 + \max(\delta_y)^2 \tag{3}$$

$$p = \left(\sum_j C_j - \sum_i C_i\right)^2 \tag{4}$$

Where $\Phi$ is the objective function, $f_{obj}$ is the fitness function, $p$ is the penalty function, $\delta_x$ and $\delta_y$ are the maximum peak inter-storey drift ratio in x and y direction, $\sum_j C_j$ is the constraint of the total damping coefficient and $\sum_i C_i$ is the total damping coefficient of one specific population.

The fitness function of each chromosome is used as criteria to calculate the probability to select the chromosome with the corresponding fitness function into the crossover pool based on RWS in each iteration.

### 4.1.3 Uniform Distribution (UD)

UD distributes damping coefficients uniformly at each storey. Based on the equivalent damping ratio, the damping coefficient contributed by linear viscous dampers at each storey can be expressed as,

$$c_i = \frac{4\pi\xi_d \sum_i m_i \varphi_i^2}{T \sum_j \varphi_{rj}^2 cos^2\theta_j} \tag{5}$$

where $\theta_i$ is the inclination angle of the damper on *i* th storey to the horizontal, $\varphi_{rj}$ is the first relative mode shape, $c_i$ is damping coefficient of the *i* th storey, *T* is the fundamental structural period.

In addition, the sum of the damping coefficients can be described as follows:

$$\sum_i c_i = C \tag{6}$$

### 4.1.4 Distribution based on Storey Shear Strain Energy (SSSE)

The concept of this distribution is the total damping coefficients is distributed according to the storey shear strain energy relationship $E_i$ at each storey. The storey shear strain energy relationship at each storey is expressed as

$$E_i \propto \varphi_{ri} \sum_{j=i}^{n} m_j \varphi_j \tag{7}$$

where $E_i$ is the storey shear strain energy of *i* th storey, *n* is the total number of storeys of the building, $m_j$ is the mass on *j* th storey and $\varphi_{ri}$ is the value of the first relative mode shape on *i* th storey.

Then, the damping coefficient distribution formula can be expressed as

$$c_i = \frac{E_i}{\sum_j E_j} C \tag{8}$$

### 4.1.5 Distribution based on Storey Shear Strain Energy to Efficient Storeys (SSSEES)

Another distribution technique that aims to make more efficient use of viscous dampers is SSSEES. In SSSEES, the total damping coefficient is distributed only to storeys with a shear strain energy larger than the average storey shear strain energy.


 

$$\varphi_{ri}S_i > \frac{\sum_{j=1}^{n}\varphi_{rj}S_j}{n} \tag{9}$$

Then, the damping coefficient distribution based on the SSSE to efficient story (SSSEES) can be derived as

$$c_i = \frac{E_i}{\sum_j E_j}C \tag{10}$$

where $i$ and $j$ are the storeys with a shear strain energy larger than the average storey shear strain energy.

### 4.1.6 Distribution Based on Energy Dissipated by Viscous Damper (EDVD)

When a MDOF system with viscous dampers is subjected to a sinusoidal excitation, the work done by those dampers in a cycle [18] can be expressed as follows

$$W_D = \sum_j W_{Dj} = \sum_j \lambda_j c_j \omega^\alpha (u_j)^{1+\alpha} = \sum_j \lambda_j c_j \omega^\alpha A^{1+\alpha} cos^{1+\alpha}\theta_j \varphi_{rj}^{1+\alpha} \tag{11}$$

Hence, the distribution formula can be expressed as

$$c_i = \frac{W_{Di}}{\sum_j W_{Dj}}C = \frac{\lambda_i c_i \omega^\alpha A^{1+\alpha} cos^{1+\alpha}\theta_i {\varphi_{ri}}^{1+\alpha}}{\lambda_j c_j \omega^\alpha A^{1+\alpha} cos^{1+\alpha}\theta_j \sum_j {\varphi_{rj}}^{1+\alpha}}C = \frac{{\varphi_{ri}}^{1+\alpha}}{\sum_j {\varphi_{rj}}^{1+\alpha}}C \tag{12}$$

where $\lambda = 2^{2+\alpha}\frac{\Gamma^2(1+\frac{\alpha}{2})}{\Gamma(2+\alpha)}$, $\Gamma$ is gamma function, $\theta_i$, $\theta_j$ is the inclination angle of the damper on $i$ th and $j$ th storey to the horizontal, respectively, $\varphi_{ri}$ is the value of first relative mode shape on $i$ th storey, $c_i$ is the damping coefficient of the $i$ th storey, $\omega$ is first mode natural frequency, $A$ is the maximum roof displacement, $\alpha$ is damping exponent which is equal to 1 in this study.

### 4.1.7 Distribution Based on Energy Dissipated by Viscous Damper to Efficient Storeys (EDVDES)

The total damping coefficient is distributed only to those storeys with a relative mode shape to the power of $\alpha$ larger than the average relative mode shape to the power of $\alpha$.

$${\varphi_{ri}}^{1+\alpha} > \frac{\sum_{j=1}^{n}{\varphi_{rj}}^{1+\alpha}}{n} \tag{13}$$

Then, the damping coefficient distribution based on the EDVD to efficient story (EDVDES) can be derived as

$$c_i = \frac{{\varphi_{ri}}^{1+\alpha}}{\sum_j {\varphi_{rj}}^{1+\alpha}}C \tag{14}$$

where $i$ and $j$ are the storeys with a storey drift larger than the average storey drift.

### 4.2 Viscous damper placement design of all methods

For all three case study buildings, the inherent damping ratio of the building is set at 5% and the total damping supplemented by linear viscous dampers is 15% equivalent viscous damping in both horizontal directions. The total damping coefficient and the damping coefficient of one damper in each case are shown in Table 3. One limitation of EEM, IEEM, SSSA and GA is that the design damper placement is sensitivity to the ground motion record. Thus, five pairs of ground motion are used for this case study. Under five pairs of ground motion, 10 damper placement design can be obtained. Some of them are identical meaning that those designs occur most frequently and can address EDPs caused by most ground motions. Finally, Denali PS12 (2002) selected herein for three case study buildings to design damper placements which can result in the most frequently occurring damper placement design is chosen for the design ground motion.



 

Table 3– The detail of added damping

| | Number of dampers in each direction | | Total damping coefficient (kN-s/m) | | Damping coefficient of one damper (kN-s/m) | |
|---|---|---|---|---|---|---|
| | **X-direction** | **Y-direction** | **X-direction** | **Y-direction** | **X-direction** | **Y-direction** |
| **Symmetric building** | 16 | 16 | 189000 | 247000 | 11800 | 15400 |
| **One-way asymmetric building** | 16 | 16 | 186000 | 249000 | 11600 | 15500 |
| **Two-way asymmetric building** | 16 | 16 | 184000 | 240500 | 11500 | 15000 |

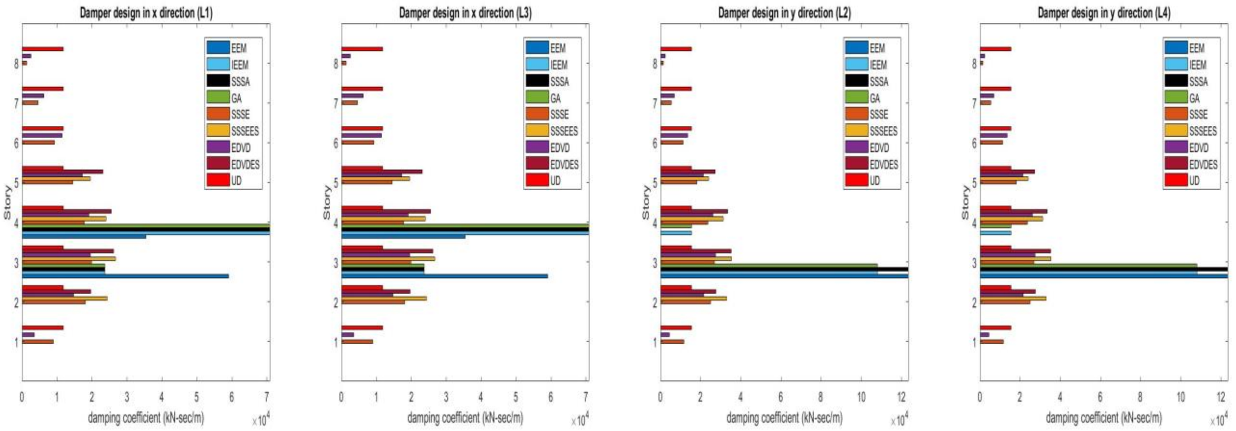


Fig. 3- Damper placement design of all methods for the symmetrical building

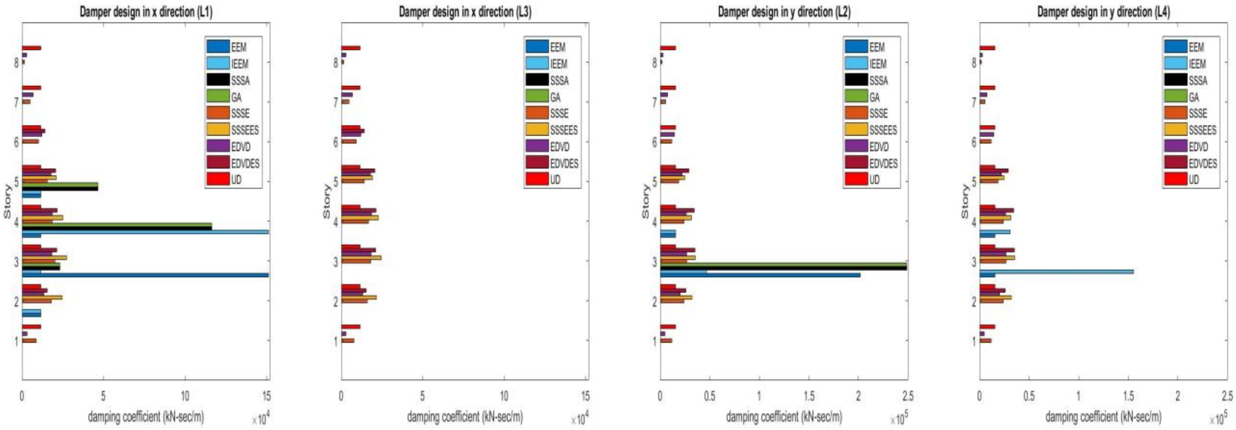


Fig. 4- Damper placement design of all methods for the one-way asymmetrical building



 

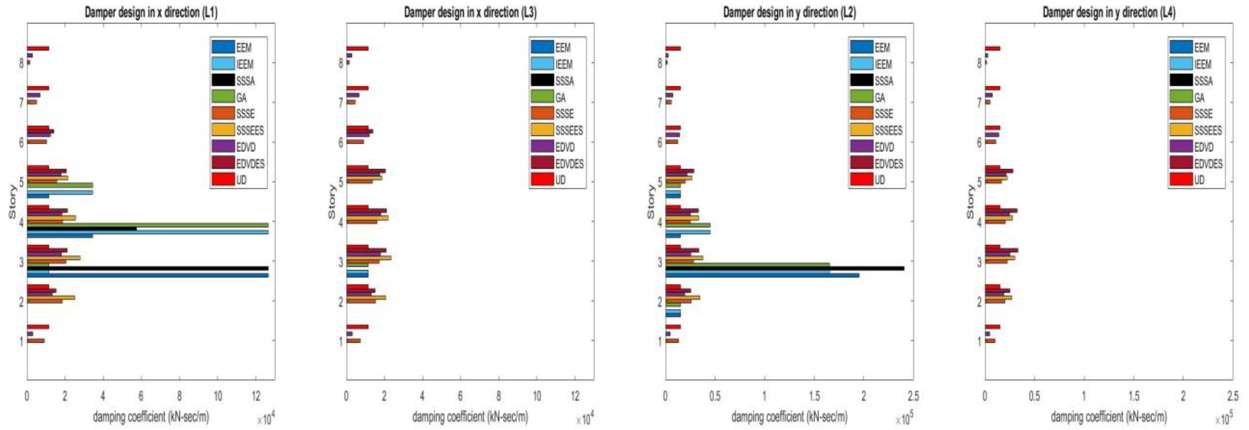


Fig. 5- Damper placement design of all methods for the two-way asymmetrical building

## 5. Results

Fig. 3- 5 show the optimum damper design from all the examined methods, they represent the designs for the symmetrical building, the one-way asymmetrical building and the two-way asymmetrical building respectively. As can be observed from Fig. 3, plan symmetry can generate symmetric damper placement between L1 and L3 in x-direction and L2 and L4 in the y-direction. On the other hand, Fig. 4 and Fig. 5 show the damper placement methods recommend concentrating the added dampers on the flexible side (i.e. L1 and L2) where the EDPs are amplified by the torsion effect. Table 4 shows the number of required iterations for a solution for each method. Table 4 highlights that asymmetrical buildings require more iteration, and EEM and IEEM require fewer iteration compared to SSSA and GA in the same case study.

Table 4– The number of iteration of methods requiring dynamic analyses

| Case | EEM | IEEM | SSSA | GA |
|---|---|---|---|---|
| Sym. bldg | 8 | 7 | 8 | 17 |
| One-way asy. bldg | 13 | 13 | 16 | 24 |
| Two-way asy. bldg | 13 | 13 | 16 | 27 |

### 5.1 Building performance comparison

Since a rigid diaphragm is assumed for the symmetrical building and there is no rotational ground motion input, the building response will be purely translational and the EDPs is identical in the same direction on any point of the plan on one specific storey. Thus, only EDPs of the centre of mass are shown in Fig. 6. Fig. 6 shows that methods requiring time history analyses and iterations produced good peak inter-storey drift ratios (IDR) in both horizontal directions. SSSEES and EDVDES effectively minimised peak floor accelerations and produced similar results to those methods requiring time history analyses. It is noteworthy that while IEEM, SSSA, GA, whose damper placements are identical in the x-direction, can effectively minimise peak IDR in the x-direction, they resulted in higher peak floor acceleration in x-direction on the top of the building.

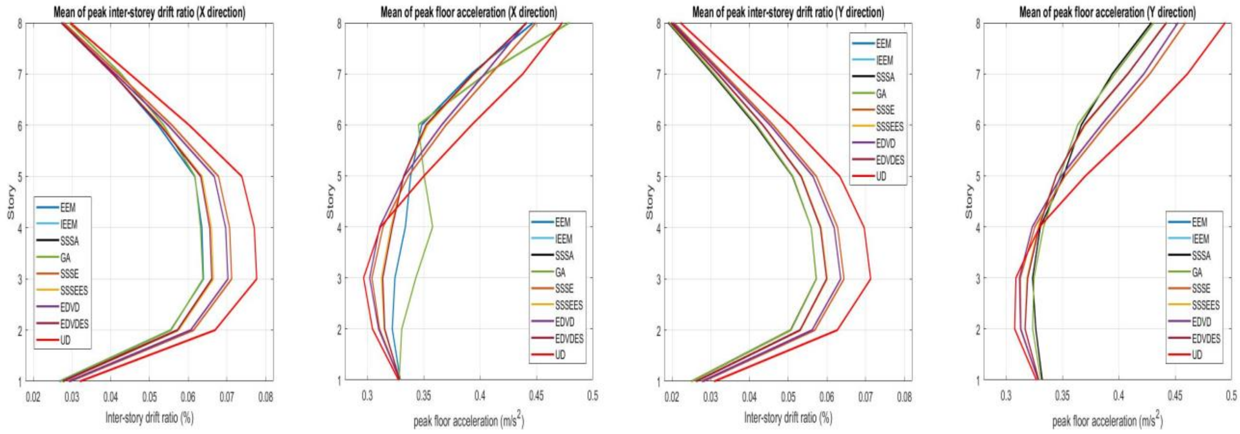


Fig. 6- Mean of peak IDR and floor acceleration of the symmetric building

Fig. 7 and Fig. 8 shows that methods requiring time history analyses and iterations successfully minimised peak inter-storey drift ratios (IDR) and peak floor accelerations (PFA) in both horizontal directions.

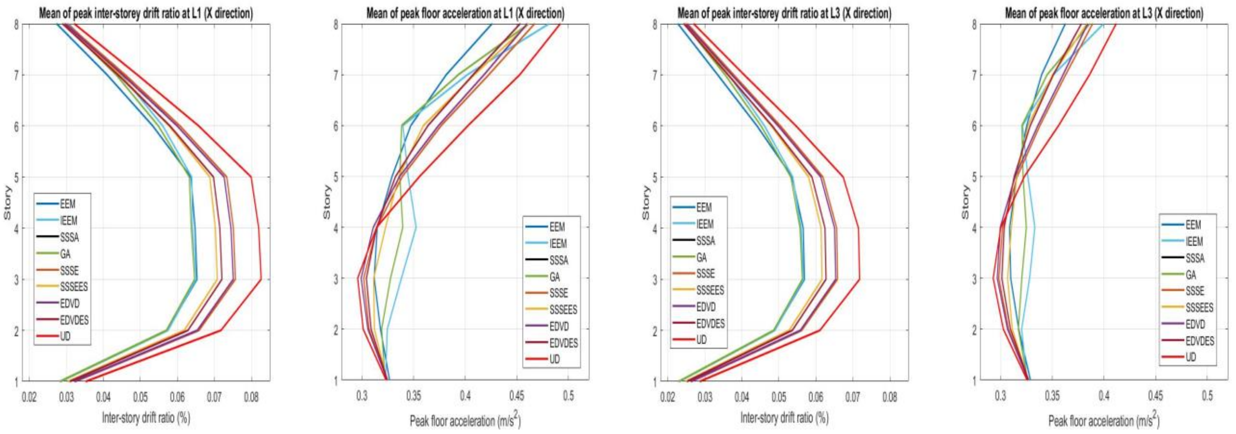


Fig. 7- Mean of peak IDR and floor acceleration in x direction of the one-way asymmetric building

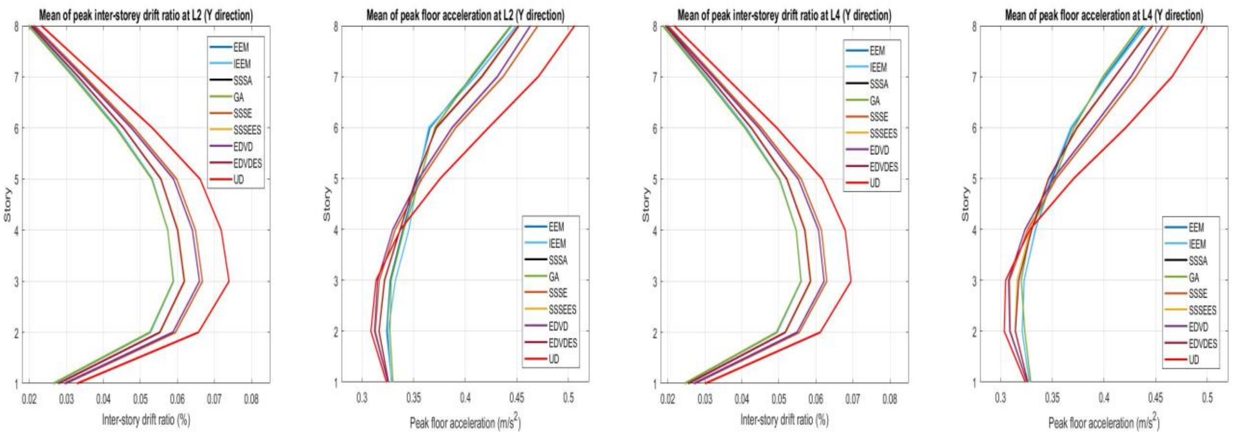


Fig. 8- Mean of peak IDR and floor acceleration in y-direction of the one-way asymmetric building

Fig. 9 and Fig. 10 demonstrate that EEM, IEEM, SSSA and GA were the most effectively in reducing both peak IDR and PFA for both flexible and stiff side of the building. These results are similar to that for the symmetric and one-way asymmetric building shown previously in Fig. 6- 8. Moreover, Fig. 10 shows that optimum damper placement can significantly correct for torsion effect in buildings. Table 5 and Table 6 show the rank of the different methods' efficiency across three different types of buildings. As can be observed, EEM and IEEM can reduce maximum mean peak EDPs as well as SSSA and GA do in three cases.

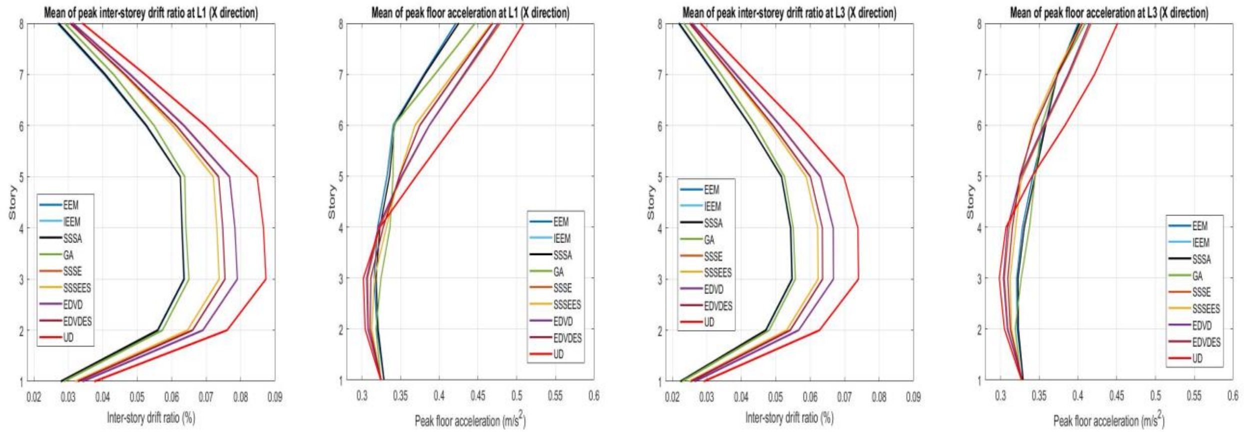


Fig. 9- Mean of peak IDR and floor acceleration in the x-direction of the two-way asymmetric building

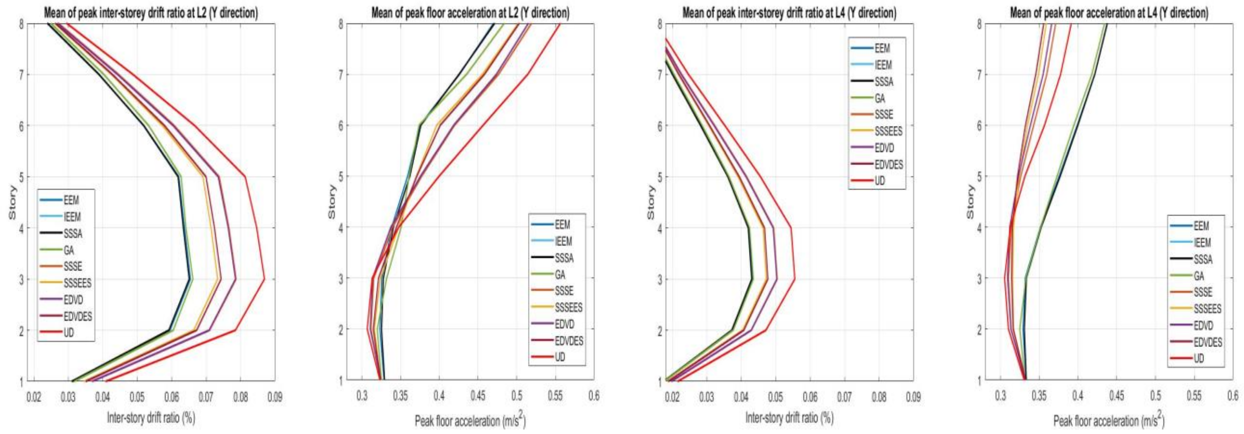


Fig. 10- Mean of peak IDR and floor acceleration in the y-direction of the two-way asymmetric building

Table 5– Reduction from max. mean peak IDR of UD

| Symmetric Building | | | One-way asymmetric building | | | Two-way asymmetric building | | |
|---|---|---|---|---|---|---|---|---|
| Rank | Method | Reduction of max. mean peak IDR (%) | Rank | Method | Reduction of max. mean peak IDR (%) | Rank | Method | Reduction of max. mean peak IDR (%) |
| 1 | EEM | 16.88 | 1 | SSSA | 21.76 | 1 | SSSA | 27.28 |
| 2 | IEEM | 16.52 | 1 | GA | 21.76 | 2 | EEM | 27.10 |
| 2 | SSSA | 16.52 | 3 | IEEM | 21.25 | 3 | IEEM | 25.57 |
| 2 | GA | 16.52 | 4 | EEM | 20.96 | 3 | GA | 25.57 |
| 5 | EDVDES | 14.47 | 5 | SSSES | 14.33 | 5 | SSSES | 15.54 |

Table 6– Reduction from max. mean PFA of UD

| Symmetric Building | | | One-way asymmetric building | | | Two-way asymmetric building | | |
|---|---|---|---|---|---|---|---|---|
| Rank | Method | Reduction of max. mean PFA (%) | Rank | Method | Reduction of max. mean PFA (%) | Rank | Method | Reduction of max. mean PFA (%) |
| 1 | IEEM | 13.65 | 1 | SSSA | 12.23 | 1 | EEM | 15.53 |
| 1 | GA | 13.65 | 1 | GA | 12.23 | 2 | SSSA | 15.27 |
| 3 | EEM | 13.60 | 3 | EEM | 12.12 | 3 | IEEM | 13.03 |
| 3 | SSSA | 13.60 | 4 | IEEM | 11.09 | 3 | GA | 13.03 |
| 5 | EDVDES | 11.17 | 5 | EDVDES | 10.71 | 5 | SSSES | 9.75 |

## 5. Conclusions

The proposed optimal algorithms and existing methods are applied to three case study buildings with varying eccentricity ratios. The study indicates that EEM and IEEM can mitigate peak inter-storey drift ratios as well as SSSA and GA and with fewer iterations in three case studies. Further, EEM, IEEM, SSSA, GA can reduce peak IDRs much more than the other methods. On the other hand, SSSEES and EDVDES still perform better than UD in all cases, and these methods do not require any iteration.

## 6. Acknowledgements

The first author gratefully acknowledges the financial support by the University of Auckland through the University of Auckland Doctoral Scholarships programme.

## 7. References

[1] Shin, H., & Singh, M. (2014). Minimum failure cost-based energy dissipation system designs for buildings in three seismic regions–Part II: Application to viscous dampers. *Engineering Structures, 74*, 275-282.
[2] Puthanpurayil, A., Lavan, O., & Dhakal, R. (2017). *Multi-objective loss optimization of seismic retrofitting of moment resisting frames using viscous dampers.* Paper presented at the Proceedings of the 16th world conference on earthquake engineering (16WCEE).
[3] Garcia, D. L. (2001). A simple method for the design of optimal damper configurations in MDOF structures. *Earthquake Spectra, 17*(3), 387-398.
[4] Levy, R., & Lavan, O. (2006). Fully stressed design of passive controllers in framed structures for seismic loadings. *Structural and Multidisciplinary Optimization, 32*(6), 485-498.
[5] Takewaki, I. (2000). Optimal damper placement for critical excitation. *Probabilistic Engineering Mechanics, 15*(4), 317-325.
[6] Takewaki, I. (1997). Optimal damper placement for minimum transfer functions. *Earthquake Engineering & Structural Dynamics, 26*(11), 1113-1124.
[7] Lopez Garcia, D., & Soong, T. (2002). Efficiency of a simple approach to damper allocation in MDOF structures. *Journal of Structural Control, 9*(1), 19-30.
[8] Whittle, J., Williams, M., Karavasilis, T., & Blakeborough, A. (2012). A comparison of viscous damper placement methods for improving seismic building design. *Journal of Earthquake Engineering, 16*(4), 540-560.
[9] Del Gobbo, G. M., Williams, M. S., & Blakeborough, A. (2018). Comparing fluid viscous damper placement methods considering total-building seismic performance. *Earthquake Engineering & Structural Dynamics, 47*(14), 2864-2886.
[10] Chan, P.-T. (2016). *Optimal Design of Viscous Dampers for Two and Three-Dimensional Building Structures.* National Taiwan University.
[11] Rouhi, M., Rais-Rohani, M., & Williams, T. N. (2010). Element exchange method for topology optimization. *Structural and Multidisciplinary Optimization, 42*(2), 215-231.
[12] Standard, N. Z. (1995). NZS 3101: Part 1 Concrete structures standard. *Pard--the Design of Concrete Structures*.
[13] Standard, N. Z. (2004). NZS 1170.5: 2004 Structural Design Actions Part 5: Earthquake actions–New Zealand. *Wellington, New Zealand: Standards New Zealand*.
[14] Book, R. (2008). Examples of Concrete Structural Design to New Zealand Standard 3101: CCANZ, Wellington, NZ.[Google Scholar].
[15] Computer and Structures Inc. (2013). *SAP2000*, version 16, Berkeley, CA.
[16] PEER. (2013). PEER NGA-WEST 2 Ground Motion Database.
[17] Hwang, J.-S., Huang, Y.-N., Yi, S.-L., & Ho, S.-Y. (2008). Design formulations for supplemental viscous dampers to building structures. *Journal of structural engineering, 134*(1), 22-31.
[18] Seleemah, A., & Constantinou, M. C. (1997). *Investigation of seismic response of buildings with linear and nonlinear fluid viscous dampers*: National Center for Earthquake Engineering Research Buffalo.



 